Dyes and Pigments 89 (2011) 199–211

Contents lists available at ScienceDirect

Dyes and Pigments

journal homepage: www.elsevier.com/locate/dyepig

The synthesis of 5,10,15,20-tetraarylporphyrins and their platinum(II) complexes as luminescent oxygen sensing materials

Wenting Wu [a], Wanhua Wu [a], Shaomin Ji [a], Huimin Guo [b], Xin Wang [c], Jianzhang Zhao [a,*]

[a] State Key Laboratory of Fine Chemicals, School of Chemical Engineering, Dalian University of Technology, 158 Zhongshan Road, P.O. Box 40, Dalian 116012, PR China
[b] Department of Chemistry, School of Chemical Engineering, Dalian University of Technology, 158 Zhongshan Road, Dalian 116012, PR China
[c] Faculty of Chemistry, Sichuan University, Chengdu 610064, PR China

ARTICLE INFO

Article history:
Received 15 November 2009
Received in revised form
25 January 2010
Accepted 27 January 2010
Available online 16 February 2010

Keywords:
Porphyrin
Luminescent oxygen sensing
DFT/TDDFT
Triplet state
Phosphorescence

ABSTRACT

5,10,15,20-tetraarylporphyrins TPP, TNP and TPyP (where TPP = 5,10,15,20-tetraphenylporphyrin, TNP = 5,10,15,20-tetranaphthalporphyrin and TPyP = 5,10,15,20-tetrapyrenyl-porphyrin) and the corresponding Pt(II) complexes were prepared. The photophysical properties of the porphyrin ligands and the Pt(II) complexes were studied using UV–vis absorption and photo-luminescence spectra; the geometry and electronic structure of the ligands and the complexes were studied via DFT/TDDFT calculations. UV–vis absorption and luminescence emission spectra showed that the added aryl groups did not contribute to the π-conjugation system of either the metal-free porphyrins or the Pt(II) complexes and, therefore, all ligands (and complexes) displayed similar photophysical properties. DFT/TDDFT calculations supported the proposed photophysical process and indicated very weak involvement of the aryl appendents in the low-lying electronic excited states. The luminescent oxygen sensing properties of the Pt(II) complexes were studied in solution as well as in polymer films (monitored via emission intensity and lifetime mode). The results demonstrated that in the case of both the pyrenyl and naphthyl groups, the oxygen sensing character of the complexes could be improved (quenching constant K_{SV} = 0.068 $Torr^{-1}$ for Pt–TNP vs. K_{SV} = 0.040 $Torr^{-1}$ for the parent complex Pt–TPP).

1. Introduction

Luminescent oxygen sensing has attracted much attention owing to its manifold applications in the chemical, biomedical, environmental and clinical sciences [1–9]. The pivotal issue of luminescent oxygen sensing is the selection of luminescent dyes with appropriate photophysical properties which can address various analytical demands, such as emission wavelength, dynamic oxygen partial pressure dynamic range, etc. Luminescent O_2 sensing can be quantitatively described by the Stern–Volmer equation (eq. (1)) [8].

$$\frac{F_0}{F} = \frac{\tau_0}{\tau} = 1 + K_D[Q] \quad (1)$$

where F_0 and τ_0 is the initial luminescent intensity and lifetime of the phosphorescent dyes in an inert atmosphere (such as N_2), F and τ are the luminescent intensity and lifetime, respectively, in the presence of O_2, K_D is the Stern–Volmer quenching constant and [Q] is the concentration of quenchers.

For heterogeneous luminescent O_2 sensing films, however, a modified Stern–Volmer or two-site model is required to study quenching because in "homogenous" polymers, the dyes reside in different microenvironments [7,8,10]. In the two-site model, the O_2-sensitive dyes are treated as two different portions and the fraction of these two portions are defined as f_1 and f_2, respectively ($f_1 + f_2 = 1$), the two portions showing different quenching constants (K_{SV1} and K_{SV2}, Eq. (2)).

$$\frac{I_0}{I} = \frac{1}{\dfrac{f_1}{1 + K_{SV1}p_{O_2}} + \dfrac{f_2}{1 + K_{SV2}p_{O_2}}} \quad (2)$$

The dyes used for luminescent O_2 sensing are usually triplet emitters with long luminescent lifetimes, such as ruthenium bipyridine complexes and the platinum porphyrin complexes [7–9]. These two families of triplet emitters display markedly different lifetimes insofar as Ru(II) complexes are usually <1 μs whereas Pt–porphyrin complexes are generally >50 μs. In order to meet the demand of various O_2 concentration ranges, dyes with a wide range of luminescent lifetimes are needed. However, it is often difficult to tune the luminescent lifetimes of fluorophores or phosphors [8,11].

* Corresponding author. Tel./fax: +86 411 3960 8007.
E-mail address: zhaojzh@dlut.edu.cn (J. Zhao).

0143-7208/$ – see front matter © 2010 Elsevier Ltd. All rights reserved.
doi:10.1016/j.dyepig.2010.01.020

Recently, the present authors noticed that the luminescent lifetime of Ru(II) polypyridine complexes can be tuned by ligand modification (via a pyrene unit) to induce new excited states which energetically approximate to the ^{3}MLCT state (metal to ligand charge transfer). Usually an aromatic appendant with a triplet excited state that is energetically close to the ^{3}MLCT state (the emissive state of the Ru complex) is introduced, whereby equilibrium of ^{3}IL (intraligand)–^{3}MLCT can be established. As a result, the ^{3}IL can act as an energy reservoir to funnel energy to the emissive state of ^{3}MLCT and the luminescent lifetime of the Ru complexes can be extended. For example, pyrene has a T_1 state energy of 2.09 eV, the same as the ^{3}MLCT state of Ru(Phen)(bpy)$_2$ (2.09 eV) [12–14]; as a result, the lifetime of a typical Ru(II) complex can be extended to 58.4 μs for a pyrene-containing Ru complex, from 0.4 μs achieved for the parent complex Ru(bpy)$_3$ [12–14]. However, the mechanism of the lifetime extension varies for different compounds and, furthermore, the detailed mechanism of this triplet–triplet energy transfer is unclear. The present authors noticed that no attempts have been made to tune the luminescent lifetimes of Pt porphyrin complexes employing a similar supramolecular photochemical approach [15].

This paper concerns the preparation of 5,10,15,20-tetraarylsubstituted porphyrins (TPP, TNP and TPyP) and their platinum complexes in order to study both their photophysical properties and luminescent O_2 sensing properties. The design rational of the porphyrin ligands and the Pt(II) complexes was to examine the effect of these aromatic groups on the emission properties of the Pt–porphyrin complexes, especially the luminescent lifetimes and so attempt to elucidate the triplet–triplet energy transfer mechanism of the porphyrin dyads. UV–Vis absorption, emission spectra and DFT/TDDFT calculations reveal that electronic communication between the aryl appendants and the porphyrin core is weak, which is supported by experimental findings. The luminescent O_2 sensing properties of the complexes were studied by monitoring the emission intensity and luminescent lifetime variation of the complexes against O_2 partial pressure. These results may prove useful for future design of porphyrin-based triplet emitters.

2. Experimental

2.1. Materials

The chemicals were used as received without further purification. $PtCl_2$ is a product of J&K Chemical LTD., Ltd. O_2 and N_2 of high purity were used in the studies.

The polymer for the fabrication of the O_2 sensing films was poly(aryl ether ketone) (IMPEK-C) (Scheme 1) [16] (Scheme 1). The number-average molecular mass ($\overline{M_n}$) of IMPEK-C is 250 460 g/mol, with a polydispersity index (PDI) of 1.94.

2.2. Characterization

NMR spectra were recorded using a 400 MHz Varian Unity Inova spectrophotometer. Mass spectra were recorded using a Q-TOF Micro MS spectrometer and MALDI micro MX. UV–Vis absorption spectra were obtained using a PerkinElmer Lambda 35 UV–Vis spectrophotometer. Emission spectra were recorded on either a JASCO FP-6500 or a Sanco 970 CRT spectrofluorometer. Fluorescence and phosphorescence quantum yields were measured using 5,10,15,20-tetraphenylporphyrin (TPP) ($\Phi = 0.11$, in benzene) and TPP-Pt ($\Phi = 0.046$, in CH_2Cl_2) as reference [17]. Fluorescence lifetime was measured using the frequency-domain instrument of Chronos 95 145 fluorescence lifetime spectrometer (ISS, Inc., Champaign, IL, USA). The regression of the experimental decay curves was carried out employing VINCI Analysis (BETA 1.6) software. The home-assembled time-domain luminescent lifetime device has been described elsewhere [7].

Typical film preparation was undertaken by dissolving 10.0 mg of IMPEK-C polymer in 0.5 mL acetone to which was added 0.2 mL of Pt porphyrin complex solution in chloroform (1.0×10^{-3} mol dm^{-3}). After thorough mixing, ~0.3 mL of the solution was applied to a silica glass disk (diameter: 1.6 cm) and the solvent was evaporated at room temperature to realize a transparent film [the thickness of the film of TPP–Pt was estimated as 22 μm, according to the mass of the film (5.1 mg) and the density of the polymer (1.14 g cm^{-3})]. Similarly the thickness of the film of TNP–Pt, and TPyP–Pt were estimated as 21 μm and 24 μm, respectively.

2.3. Theoretical calculations

The structure of the porphyrins and the Pt complexes were optimized using density functional theory (DFT) with B3LYP functional and the 6-31G (d)/LanL2DZ basis set. The excited state related calculations were carried out employing time dependent DFT (TD-DFT) with optimized ground state geometry. The 6-31G (d) basis set was employed for C, H, N and the LanL2DZ basis set was used for Pt (II). There were no imaginary frequencies for any of the optimized structures. All calculations were performed with Gaussian 09 [18].

2.4. Synthesis of 5,10,15,20-tetrakisphenylporphyrin (TPP)

The compound was prepared by a reported method [19]. ^{1}H NMR (400 MHz, $CDCl_3$) δ 8.84 (s, 8H), 8.20 (d, 8H, $J = 8.0$ Hz), 7.79–7.71 (m, 12H), −2.76 (s, 2H). ESI-MS m/z: calcd for $C_{44}H_{30}N_4$ ($[M + H]^+$) 614.2471, found 615.0590.

2.5. Synthesis of platinum complex of 5,10,15,20-tetrakisphenylporphyrinTPP (Pt–TPP)

$PtCl_2$ (caution:deliquescent; protect from moisture; protect from light; 37.0 mg, 0.14 mmol) was added to 35 mL benzonitrile and the mixture was refluxed for 4 h, after which time, $PtCl_2$ was completely dissolved in benzonitrile and 5,10,15,20-tetraphenylporphyrin (28.0 mg, 0.046 mmol) was added to the solution. The system was refluxed for 2 h. Benzonitrile (35 mL) was removed under reduced pressure and the crude product was purified using column chromatography (silica gel, $CHCl_3$). A red solid was obtained (30.0 mg, 81.7%). ^{1}H NMR (400 MHz, $CDCl_3$) δ 8.75 (s, 8H), 8.14 (d, 8H, $J = 8.0$ Hz), 7.75–7.72 (m, 12H). HR MALDI-MS m/z: calcd for $C_{44}H_{28}N_4Pt$ ($[M]^+$) 807.1962, found 807.1922.

2.6. Synthesis of pyrene-1-carbaldehyde [20]

Under an Ar atmosphere, pyrene (6.06 g, 29.8 mmol), dry chloroform (22.5 mL) and *N*,*N*-dimethylformamide (4.6 mL) were mixed and stirred for 10 min. After pyrene had dissolved, $POCl_3$ (caution: Reacts violently with water; incompatible with many metals, alcohols, amines, phenol, DMSO, strong bases; 9.2 g, 60.4 mmol) was added while the reaction mixture was cooled with ice/water. The ensuing solution was stirred at 60 °C for 20 h after which time, the reaction mixture was concentrated by evaporation and then saturated sodium acetate solution was added. The precipitated solid was filtered and washed with water and then dried under vacuum. The crude product was purified by column chromatography (silica gel, petroleum ether: $CH_2Cl_2 = 1{:}1$, V/V). A yellow powder was obtained (0.64 g, 2.78 mmol, 9.3%). ^{1}H NMR (400 M Hz, $CDCl_3$) δ 7.95–8.04 (m, 2H), 8.11–8.13 (m, 2H), 8.18–8.22 (m, 3H), 8.30 (d, 1H, $J = 8.0$ Hz), 9.27 (d, 1H, $J = 12.0$ Hz), 10.68 (s, 1H). EI-MS m/z: calcd for $C_{17}H_{11}O$ ($[M + H]^+$) 231.0810, found 231.0723.

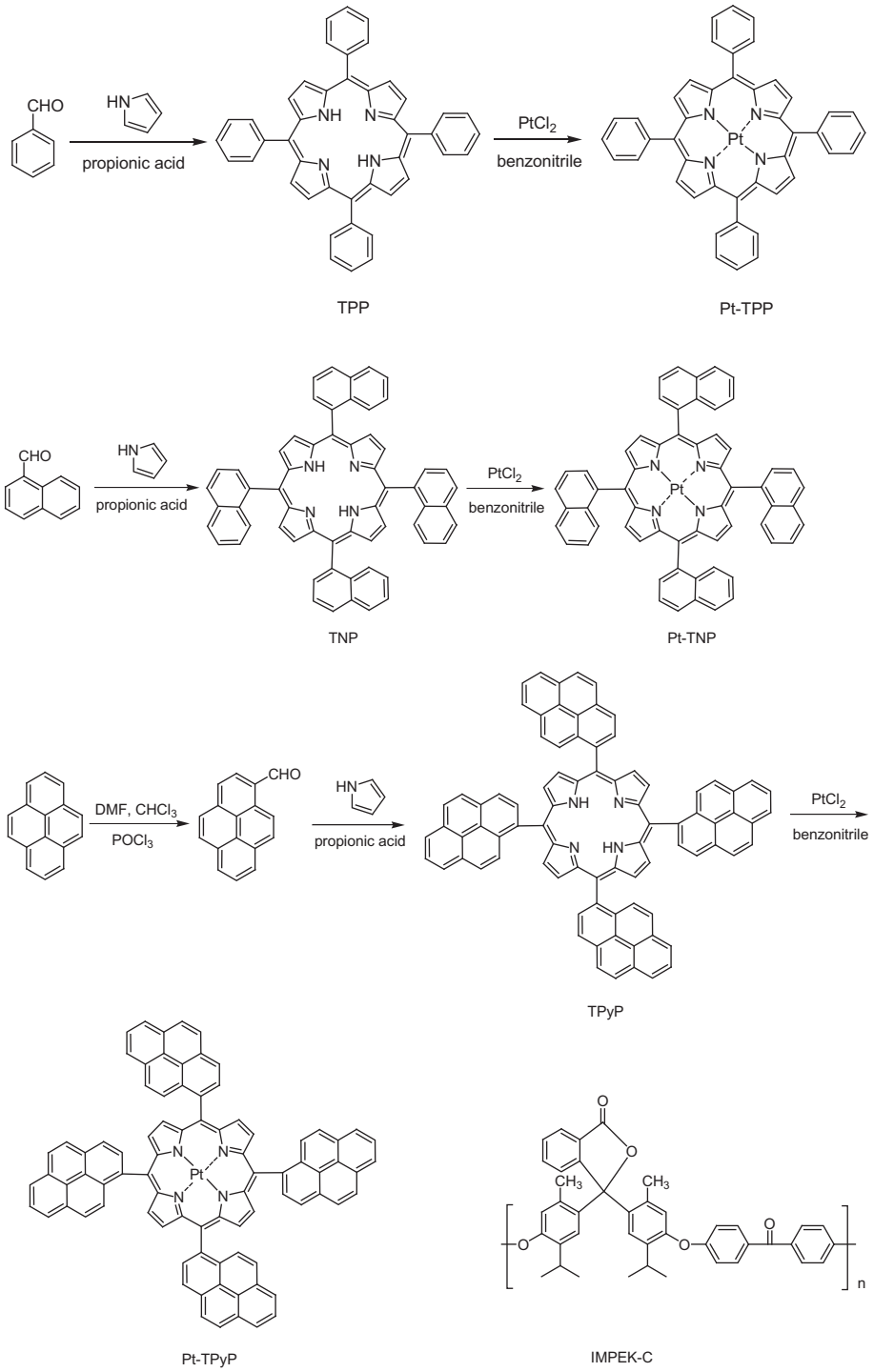

Scheme 1. Synthesis of the meso-substituted porphyrins TPP, TNP and TPyP, and the corresponding Pt(II) complexes. The polymer (IMPEK-C) used as supporting matrix for the oxygen sensing was also shown.

2.7. Synthesis of 5,10,15,20-tetrakispyrenylporphyrin (TPyP) [21]

Pyrene-1-carbaldehyde (0.46 g, 2.0 mmol) was dissolved in propionic acid (5.0 mL). The mixture was heated to reflux and freshly distilled pyrrole (0.15 g, 0.14 mL, 2.2 mmol) in propionic acid (1.5 mL) was then slowly added. After refluxing for 30 min, the solution was cooled to room temperature and filtered, the solid being washed thoroughly with ethanol. The crude product was purified by column chromatography (silica gel, CH_2Cl_2: petroleum ether = 1:1, V/V). A purple solid was obtained (66.0 mg, 12.0%). ^{1}H NMR (400 MHz, $CDCl_3$) δ 8.87–8.76 (m, 4H), 8.48–8.40 (m, 12H), 8.34 (d, 4H, J = 8.8 Hz,), 8.30–8.25 (m, 8H), 8.08–8.01 (m, 8H), 7.77–7.71 (m, 4H), 7.65–7.55 (m, 4H), −1.95 (s, 2H). ESI-MS m/z: calcd for $C_{84}H_{46}N_4$ ($[M + H]^+$) 1111.3801, found 1111.3021.

2.8. Synthesis of platinum complex of 5,10,15,20-tetrakispyrenylporphyrin (Pt–TPyP)

$PtCl_2$ (39.7 mg, 0.15 mmol) was added to 35 mL benzonitrile, the mixture was refluxed for 4 h. After $PtCl_2$ had completely dissolved

in benzonitrile, TPyP (55.5 mg, 0.05 mmol) was added and the mixture was refluxed for a further 2 h. Benzonitrile was distilled from the mixture; the crude product was purified by column chromatography (silica gel, $CHCl_3$). A red solid was obtained (20.0 mg, 30.7%). ^{1}H NMR (400 MHz, $CDCl_3$) δ 8.82–8.65 (m, 4H), 8.43–8.22 (m, 12H), 8.06–7.97 (m, 8H), 7.76–7.65 (m, 4H), 7.61–7.36 (m, 4H), 7.65–7.55 (m, 4H). HR MALDI-MS *m*/*z*: calcd for $C_{84}H_{44}N_4Pt$ ($[M]^+$) 1303.3214, found 1303.3297.

2.9. Synthesis of 5,10,15,20-tetrakisnaphtalporphyrin (TNP) [22]

The compound was synthesized following a published method [22]. Purple solid was obtained (172.0 mg, 13.2%). ^{1}H NMR (400 MHz, $CDCl_3$) δ 8.46 (s, 8H), 8.27–8.19 (m, 8H), 8.05 (d, 4H, J = 8.0 Hz), 7.77 (t, 4H, J = 7.2 Hz), 7.42 (t, 4H, J = 7.6 Hz), 7.10–7.04 (m, 4H), −2.22 (s, 2H). ESI-MS *m*/*z*: calcd for $C_{60}H_{38}N_4$ ($[M + H]^+$) 815.3175, found 815.5140.

2.10. Synthesis of platinum complex of 5,10,15,20-tetrakisnaphtalporphyrin (Pt–TNP) [22]

The compound was synthesized following a reported method [22]. A red solid was obtained (8.8 mg, 19.0%). ^{1}H NMR (400 MHz, $CDCl_3$) δ 8.41–8.38 (m, 8H), 8.28–8.21 (m, 8H), 8.09 (d, 4H, J = 8.4 Hz), 7.81 (t, 4H, J = 7.6 Hz), 7.46 (t, 4H, J = 6.8 Hz), 7.15–7.07 (m, 8H). HR MALDI-MS *m*/*z*: calcd for $C_{60}H_{36}N_4Pt$ ($[M]^+$) 1007.2588, found 1007.2523.

3. Results and discussion

3.1. Synthesis of the ligands and the complexes

The typical Alder-Longo method was used in the synthesis of the meso-tetrakis substituted porphyrins, with benzaldehyde, 1-naphthalaldehyde and 1-pyrenealdehyde [23]. The substituted porphyrins were prepared with satisfying yields (12–17%). The free ligands were metalated by $PtCl_2$ with benzonitrile as the solvents. The Pt complexes of the porphyrins were purified with column chromatography and pure compounds were obtained, verified by ^{1}H NMR and HR MS spectra.

3.2. Photophysical properties

The UV–Vis absorption spectra and emission spectra of the tetraarylporphyrins and the Pt complexes were studied (Fig. 1). The intensive absorption of the ligands at 400 nm is due to the Soret band (B band, $S_0 \rightarrow S_3$ transition) [23,24], and the weak absorption at 500 nm and 600 nm is the Q band ($S_0 \rightarrow S_1$ and $S_0 \rightarrow S_2$ transitions). The assignments of the absorption of the porphyrins were supported by our DFT/TDDFT calculations (vide infra). With different aryl substitution, the UV–Vis absorption spectra show only minor changes (Fig. 1). The molar extinction coefficients at the peak position decreased with introduce of naphthyl and pyrenyl substituents [25]. Metalated porphyrins show the similar UV–Vis absorption changes (Fig. 1b). For the Pt complexes, the minor absorption band of the free ligands at 550 nm–650 nm disappeared (Fig. 1b).

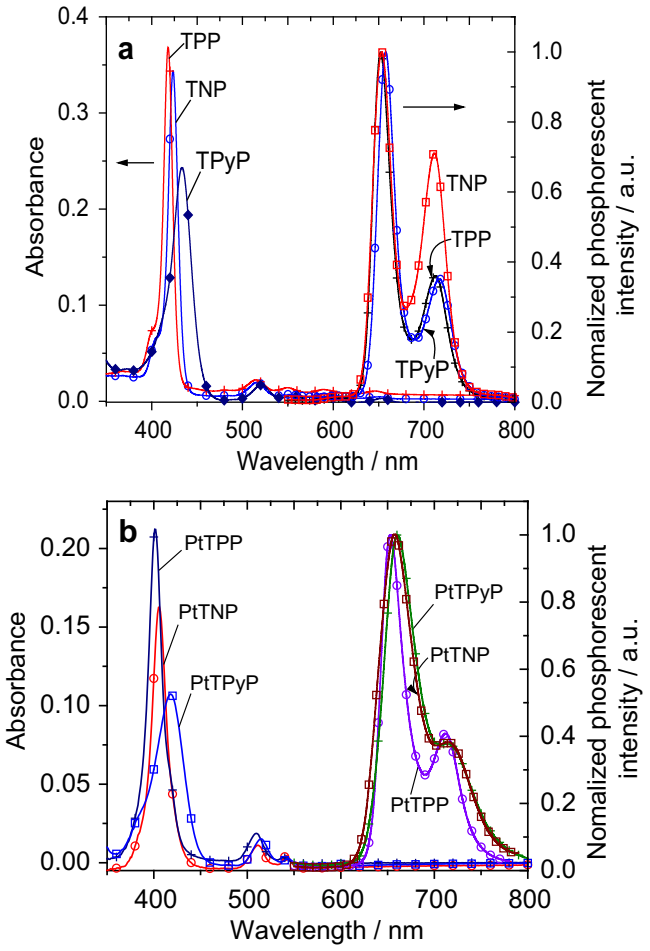

Fig. 1. Absorption and normalized emission spectra of (a) porphyrins TPP, TNP and TPyP ($c = 1 \times 10^{-5}$ mol/L) and (b) Pt porphyrin complexes Pt–TPP, Pt–TNP and Pt–TPyP in deaerated chloroform solution ($c = 2.0 \times 10^{-6}$ mol/L). 27 °C.

The free porphyrin ligands show intensive red emission in the range of 650–750 nm (Fig. 1a). The ligands were excited at different wavelengths, including the absorption of the appendents, such as the naphthylene and pyrene, however, only the emission of porphyrin core was observed, which indicates efficient singlet energy transfer within these dyad fluorophores (see Supporting Information) [8,26]. The similar emission profile of the free porphyrins indicate that the pyrene group failed to impart

Table 1
Photophysical properties of porphyrin and Pt porphyrin (in chloroform).

	λex (nm)[a]	λem (nm)[a]	abs[a]	Φ[a]	τ
Pt–TPP	425	653	402 (2.22), 510 (0.16), 539 (0.04)	0.046	56.8 ± 1.2[b]
Pt–TNP	407	658	275 (0.25), 406 (1.63), 511 (0.11), 543 (0.07)	0.037	78.1 ± 0.6[b]
Pt–TPyP	432	663	326 (0.28), 341 (0.29), 418 (1.07), 515 (0.17), 544 (0.05)	0.051	66.7 ± 0.9[b]
TPP	425	652	418 (4.76), 515 (0.13), 550 (0.08), 590 (0.06)	0.110	9.1 ± 0.0[c]
TNP	430	653	275 (0.29), 424 (3.46), 516 (0.16), 590 (0.06)	0.076	10.0 ± 0.0[c]
TPyP	441	657	326 (0.45), 341 (0.42), 434 (2.43), 521 (0.21), 556 (0.09)	0.130	10.1 ± 0.0[c]

[a] Measurements were performed in chloroform solvent and extinction coefficients (ε, $\times 10^5$ M^{-1} cm^{-1}) are shown in parentheses. Fluorescence and phosphorescence quantum yields were measured with 5,10,15,20-tetraphenylporphyrin (TPP) (Φ = 0.11, in benzene) and Pt -TPP (Φ = 0.046, in CH_2Cl_2) as the reference [17].
[b] Phosphorescence lifetime (μs) of sensing film of Pt porphyrin in IMPEK-C in neat N_2 recorded with the home-assembled lifetime device.
[c] Fluorescence lifetime (ns) of porphyrin in $CHCl_3$.

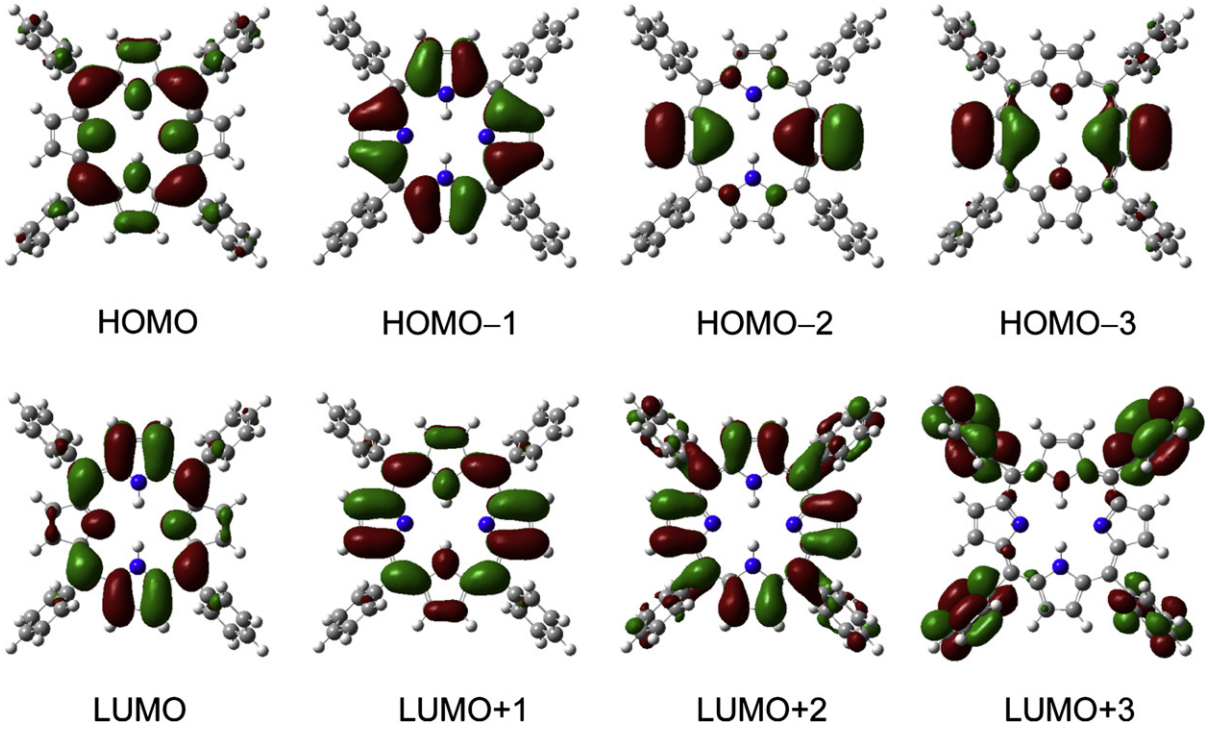

Fig. 2. Frontier molecular orbitals of the tetrakisphenyl porphyrin (TPP). Calculated at the DFT//B3LYP/6-31G(d) level.

influence on the photophysical properties of the porphyrin core, i.e. the electronic communication between the aryl appendents and the porphyrin core is poor [24].

All the Pt complexes show similar emission profile. Notably the Pt–TPyP shows similar emission profile to the Pt–TPP, thus, no ligand-centered emission (such as ^{3}LC, due to the $^3\pi$–π^* transition of the pyrene group) was observed [12,27–29]. We propose all of the three complex will give similar photophysical properties, i.e. the emission is due to the ^{3}LC state of the porphyrin core, not the ^{3}IL of the aryl appendents [12]. This finding is different from the photochemical feature of Ru(II) polypyridine complexes with pyrene appendents, which show ^{3}IL/^{3}LLCT emission [12,27–29].

The photophysical properties of the aryl porphyrins and the Pt complexes were summarized in Table 1. It was found the absorption and emission properties of the porphyrin don't show drastic change with variation of the aryl appendents. Also no substantial changes were observed for the emission of the complexes with different aryl appendents, for example the lifetimes of the complexes are close to

Table 2
Selected electronic excitation energies (eV) and corresponding oscillator strengths (*f*), main configurations and CI Coefficients of the low-lying electronically excited states of tetrakisphenylporphyrin (TPP), Calculated by TDDFT//B3LYP/6-31G(d), based on the DFT//B3LYP/6-31G(d) optimized ground state geometries.

	Electronic transition[a]	TDDFT//B3LYP/6-31G(d)				
		Energy	*f*[b]	Composition[c]	CI[d]	Character
Singlet	$S_0 \rightarrow S_1$	2.16 eV/575 nm	0.0188	H − 1 → L	0.4499	LC
				H → L + 1	0.5676	LC
	$S_0 \rightarrow S_2$	2.31 eV/538 nm	0.0343	H − 3 → L + 1	0.4484	LC
				H → L	0.5416	LC
	$S_0 \rightarrow S_3$	3.17 eV/391 nm	0.8021	H − 3 → L + 1	0.3485	LC
				H − 1 → L	0.4219	LC
				H → L + 1	0.2540	LC
	$S_0 \rightarrow S_4$	3.29 eV/377 nm	1.3076	H − 3 → L	0.1710	LC
				H − 1 → L + 1	0.4400	LC
				H → L	0.3103	LC
Triplet[e]	$S_0 \rightarrow T_1$	1.37 eV/908 nm	0.0000	H − 1 → L + 1	0.3593	LC
				H → L	0.7981	LC
	$S_0 \rightarrow T_2$	1.67 eV/741 nm	0.0000	H − 1 → L	0.1387	LC
				H → L + 1	0.7724	LC
	$S_0 \rightarrow T_3$	1.98 eV/625 nm	0.0000	H − 1 → L + 1	0.6998	LC
				H → L	0.2558	LC
	$S_0 \rightarrow T_4$	2.02 eV/612 nm	0.0000	H − 1 → L	0.7443	LC
	$S_0 \rightarrow T_5$	2.79 eV/444 nm	0.0000	H − 3 → L + 2	0.2139	LC
				H − 2 → L + 1	0.6972	LC

[a] Only the selected low-lying excited states are presented.
[b] Oscillator strength.
[c] H stands for HOMO and L stands for LUMO. Only the main configurations are presented.
[d] The CI coefficients are in absolute values.
[e] No spin-orbit coupling effect was considered, therefore the oscillator strength is zero.

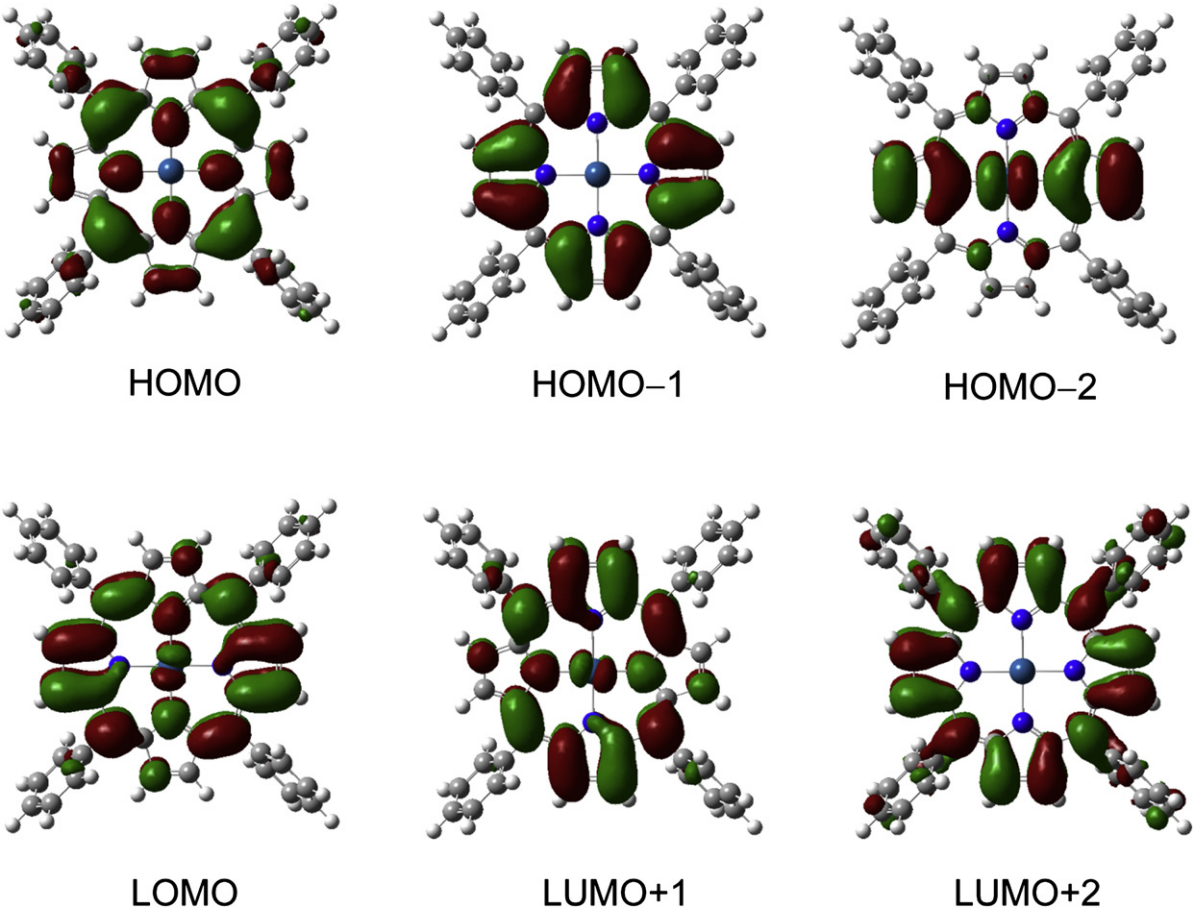

Fig. 3. Frontier molecular orbitals of the 5,10,15,20-tetrakisphenyl porphyrin (Pt–TPP). Calculated at the DFT//B3LYP/6-31G(d)/LanL2DZ level.

each other. These results may indicate that there is no significant electronic interaction between the aryl appendents and the porphyrin core. As the room temperature luminescent lifetime of pyrene is 1.74 ms [30], but Pt–TPyP shows a lifetime of 66.7 μs, no significant lifetime extension was observed when compared to the reference complex Pt–TPP [31].

3.3. Theoretical calculations

Recently DFT/TDDFT theoretical calculations have been successfully used to describe the photophysical properties of fluorophores [12,32–38]. Herein we carried out preliminary theoretical calculations to reveal the photophysical properties of the porphyrins and the

Table 3
Selected Electronic Excitation Energies (eV) and Corresponding Oscillator Strengths (*f*), Main Configurations and CI Coefficients of the Low-lying Electronically Excited States of Pt–TPP. Calculated by TDDFT//B3LYP/6-31G(d), Based on the DFT//B3LYP/6-31G(d) Optimized Ground State Geometries.

	Electronic transition[a]	TDDFT//B3LYP/6-31G(d)				
		Energy	*f*[b]	Composition[c]	CI[d]	Character
Singlet	$S_0 \rightarrow S_1$	2.55 eV/487 nm	0.0057	H − 1 → L + 1	0.4860	LC&LMCT
				H → L	0.5221	LC&LMCT
	$S_0 \rightarrow S_2$	2.55 eV/487 nm	0.0052	H − 1 → L	0.4872	LC&LMCT
				H → L + 1	0.5210	LC&LMCT
	$S_0 \rightarrow S_9$	3.38 eV/367 nm	1.0827	H − 1 → L + 1	0.4309	LC&LMCT
				H → L	0.3740	LC&LMCT
	$S_0 \rightarrow S_{10}$	3.38 eV/367 nm	1.0829	H − 1 → L	0.4295	LC&LMCT
				H → L + 1	0.3757	LC&LMCT
Triplet[e]	$S_0 \rightarrow T_1$	1.91 eV/650 nm	0.0000	H − 1 → L + 1	0.3039	LC&LMCT
				H → L	0.7302	LC&LMCT
	$S_0 \rightarrow T_2$	1.91 eV/649 nm	0.0000	H − 1 → L	0.3075	LC&LMCT
				H → L + 1	0.7286	LC&LMCT
	$S_0 \rightarrow T_3$	2.25 eV/551 nm	0.0000	H − 1 → L	0.6846	LC&LMCT
				H → L + 1	0.2584	LC&LMCT

[a] Only the selected low-lying excited states are presented.
[b] Oscillator strength.
[c] H stands for HOMO and L stands for LUMO. Only the main configurations are presented.
[d] The CI coefficients are in absolute values.
[e] No spin-orbit coupling effect was considered, therefore the oscillator strength is zero.

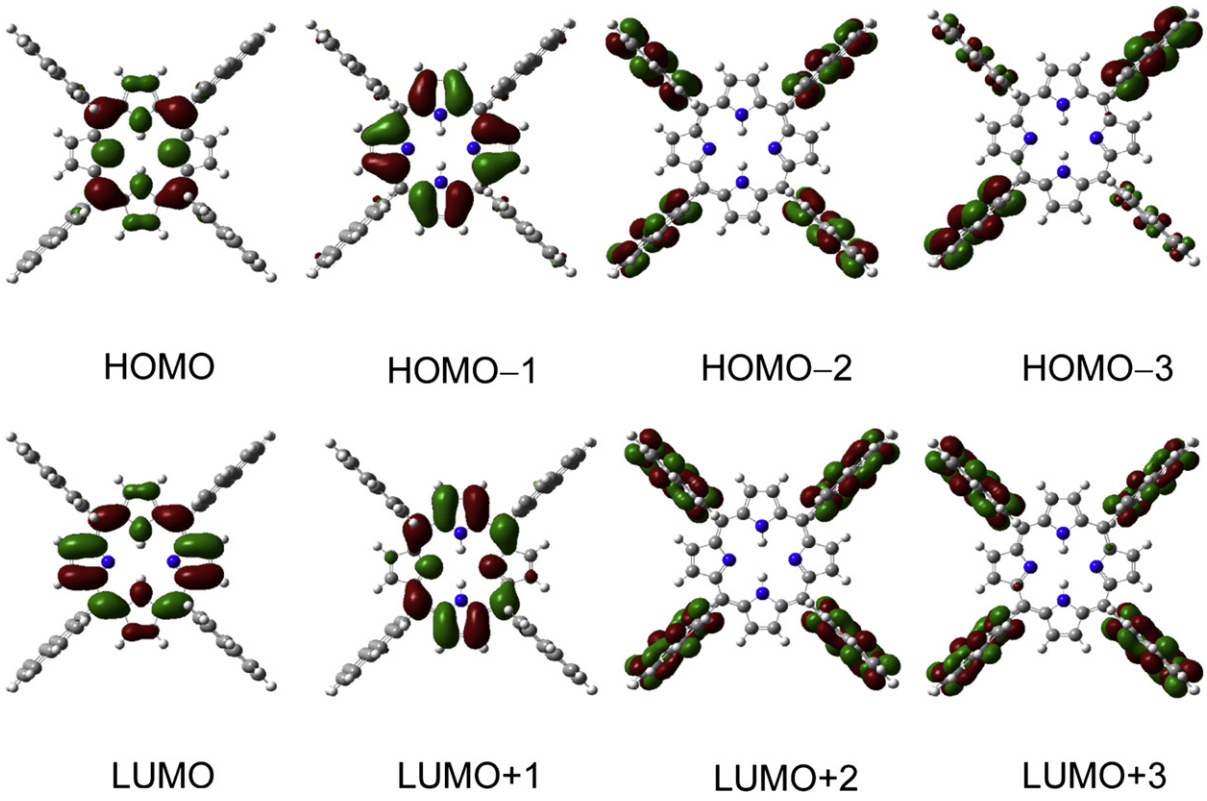

Fig. 4. Frontier molecular orbitals of the 5,10,15,20-tetrakispyrene porphyrin (TPyP). Calculated at the DFT//B3LYP/6-31G(d) level.

Table 4
Selected electronic excitation energies (eV) and corresponding oscillator strengths (*f*), main configurations and CI Coefficients of the low-lying electronically excited states of tetrakispyreneporphyrin (TPyP). Calculated by TDDFT//B3LYP/6-31G(d), Based on the DFT//B3LYP/6-31G(d) Optimized Ground State Geometries.

	Electronic Transition	TDDFT//B3LYP/6-31G(d)				
		Energy[a]	*f*[b]	Composition[c]	CI[d]	Character
Singlet	$S_0 \rightarrow S_1$	2.21 eV/561 nm	0.0177	H − 1 → L + 1	0.4329	LC
				H → L	0.5659	LC
	$S_0 \rightarrow S_2$	2.38 eV/522 nm	0.0259	H − 1 → L	0.4495	LC
				H → L + 1	0.5299	LC
	$S_0 \rightarrow S_3$	2.69 eV/462 nm	0.0048	H − 5 → L + 1	0.2792	LC
				H − 2 → L	0.6256	LLCT
				H − 1 → L + 1	0.1349	LC
	$S_0 \rightarrow S_{11}$	3.10 eV/401 nm	0.2649	H − 1 → L + 1	0.2182	LC
				H → L	0.1597	LC
				H → L + 3	0.5729	LLCT
	$S_0 \rightarrow S_{12}$	3.10 eV/400 nm	0.2335	H − 1 → L	0.1654	LC
				H → L + 5	0.6269	LLCT
	$S_0 \rightarrow S_{15}$	3.16 eV/392 nm	0.8688	H − 1 → L + 1	0.3188	LC
				H → L + 3	0.3747	LLCT
	$S_0 \rightarrow S_{16}$	3.27 eV/379 nm	1.3907	H − 1 → L	0.3122	LC
				H − 1 → L + 3	0.3357	LLCT
				H → L + 1	0.2413	LC
				H → L + 5	0.2659	LC
Triplet[e]	$S_0 \rightarrow T_1$	1.41 eV/878 nm	0.0000	H − 1 → L	0.3520	LC
				H → L + 1	0.7897	LC
	$S_0 \rightarrow T_2$	1.73 eV/715 nm	0.0000	H − 1 → L + 1	0.1225	LC
				H → L	0.7673	LC
	$S_0 \rightarrow T_3$	1.98 eV/625 nm	0.0000	H − 1 → L	0.6638	LC
				H → L + 1	0.2714	LC
	$S_0 \rightarrow T_4$	2.02 eV/612 nm	0.0000	H − 1 → L	0.7443	LC
	$S_0 \rightarrow T_5$	2.08 eV/596 nm	0.0000	H − 1 → L + 1	0.7125	LC

[a] Only the selected low-lying excited states are presented.
[b] Oscillator strength.
[c] H stands for HOMO and L stands for LUMO. Only the main configurations are presented.
[d] The CI coefficients are in absolute values.
[e] No spin-orbit coupling effect was considered, therefore the oscillator strength is zero.

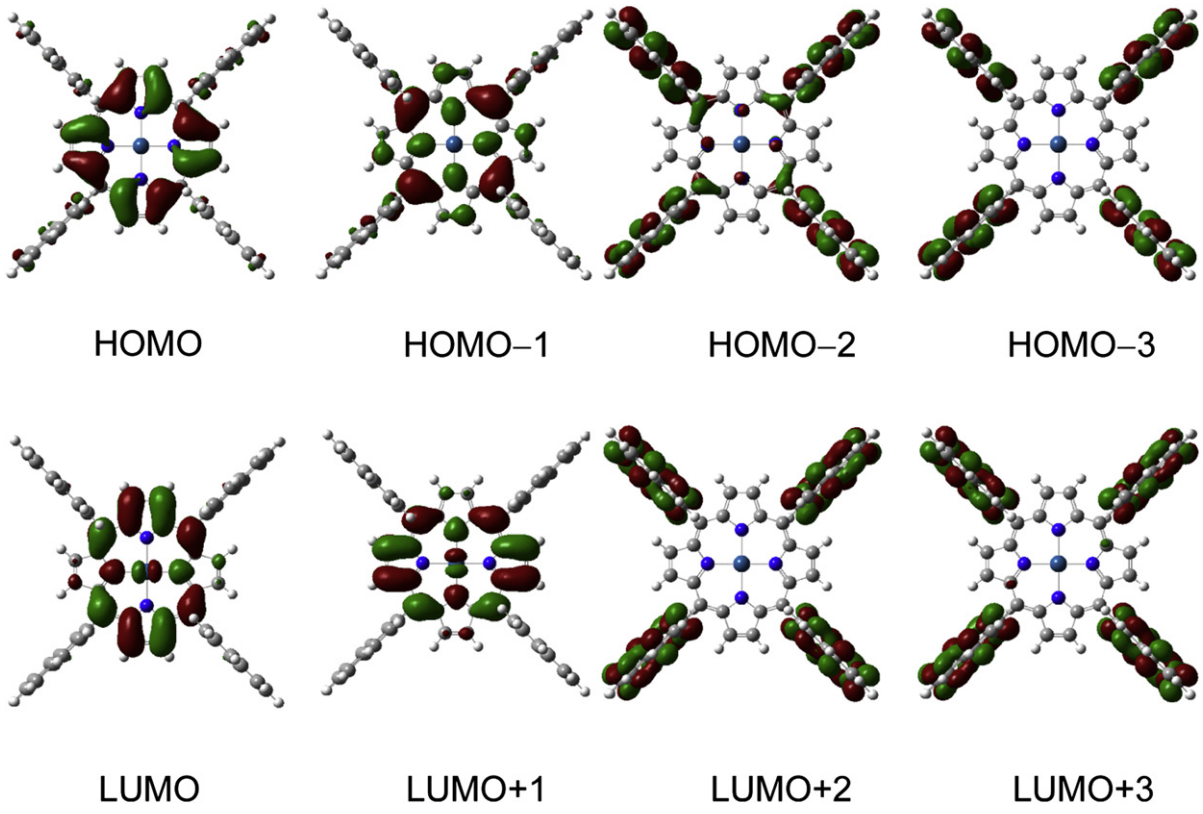

Fig. 5. Frontier molecular orbitals of the Pt complex of 5,10,15,20-tetrakispyrene porphyrin (Pt–TPyP). Calculated at the DFT//B3LYP/6-31G(d)/LanL2DZ level.

Pt complexes. Our theoretical studies focus on the geometries of the ligands/Pt-complexes, electronic transitions and the emissive state of the ligands and the Pt complexes.

As a reference compound, the geometry of TPP at the ground state was optimized. We found the porphyrin core adopts a planar geometry, which leads to an extended π-conjugation framework (Fig. 2), results in red-shifted emission at long wavelength of the fluorescence. For the phenyl appendents, however, it adopts a geometry which is nearly perpendicular (ca. 68°) to the porphyrin core. This configuration rules out any

Table 5
Selected electronic excitation energies (eV) and corresponding oscillator strengths (*f*), main configurations and CI coefficients of the low-lying electronically excited states of the Pt complex of tetrakispyreneporphyrin (Pt–TPyP). Calculated by TDDFT//B3LYP/6-31G(d), Based on the DFT//B3LYP/6-31G(d) optimized ground state geometries.

	Electronic transition	TDDFT//B3LYP/6-31G(d)				
		Energy[a]	*f*[b]	Composition[c]	CI[d]	Character
Singlet	$S_0 \rightarrow S_1$	2.50 eV/496 nm	0.0015	H − 2 → L + 1	0.1980	LLCT&LMCT
				H − 1 → L + 1	0.4157	LC&LMCT
				H → L	0.4948	LC&LMCT
	$S_0 \rightarrow S_2$	2.50 eV/496 nm	0.0008	H − 2 → L	0.1906	LLCT&LMCT
				H − 1 → L	0.4216	LC&LMCT
				H − 1 → L	0.4932	LC&LMCT
	$S_0 \rightarrow S_{15}$	3.21 eV/386 nm	1.1976	H − 1 → L	0.2753	LC&LMCT
				H → L + 1	0.2964	LC&LMCT
				H → L + 3	0.2920	LLCT
	$S_0 \rightarrow S_{16}$	3.21 eV/386 nm	1.1725	H − 1 → L + 1	0.2777	LC&LMCT
				H → L	0.2971	LC&LMCT
				H → L + 5	0.3116	LLCT
	$S_0 \rightarrow S_{25}$	3.38 eV/367 nm	0.3683	H − 1 → L + 3	0.5562	LLCT
				H → L + 5	0.2399	LLCT
Triplet[e]	$S_0 \rightarrow T_1$	1.91 eV/650 nm	0.0000	H − 2 → L	0.2789	LLCT&LMCT
				H − 1 → L	0.5669	LC&LMCT
				H → L + 1	0.4613	LC&LMCT
	$S_0 \rightarrow T_2$	1.91 eV/650 nm	0.0000	H − 2 → L + 1	0.2867	LLCT&LMCT
				H − 1 → L + 1	0.5613	LC&LMCT
				H → L	0.4634	LC&LMCT

[a] Only the selected low-lying excited states are presented.
[b] Oscillator strength.
[c] H stands for HOMO and L stands for LUMO. Only the main configurations are presented.
[d] The CI coefficients are in absolute values.
[e] No spin-orbit coupling effect was considered, therefore the oscillator strength is zero.

full π-conjugation between the porphyrin core and the phenyl appendents [32].

Based on the ground state geometries, the electronic configuration of the low-lying excited states were investigated (Table 2). The main singlet excited states infers UV–Vis absorptions band at 575 nm, 538 nm and 391 nm, which are in good agreement with the experimental observations (Fig. 1a. UV–Vis absorptions at 590 nm, 550 nm and 418 nm respectively). These results validate our theoretical calculations. The low-lying triplet state of the TPP was also investigated with the DFT/TDDFT methods. By examination of the molecular orbits, for example, the phenyl localized LUMO + 3 is not involved in the low-lying excited states, neither the singlet nor the triplet states (Table 2). We found the phenyl appendents do not involve in the transitions (Table 2 and Fig. 2).

The Pt–TPP complex was also investigated with the similar DFT/TDDFT calculations (Fig. 3 and Table 3). We found the metalation induce no perturbation to the geometry of the ligands, i.e. the porphyrin core adopts a planar geometry and the phenyl appendents tilted ca. 70° against the porphyrin core (Fig. 3).

The electronic structure of the Pt–TPP complex was investigated and we found the UV–Vis absorption of the TPP ligand at the red-end of the spectra disappeared, which is in agreement with the experimental results (Fig. 1b). By examination of the MOs and the electronic structure of the excited states (Fig. 3 and Table 3), we found that the phenyl appendents do not contribute to the molecular orbitals of the Pt–TPP complex. The triplet states were also studied and similar results were obtained [32]. We also found that Pt metal makes minor contribution to the MOs, which is consistent to the fact that Pt porphyrins complexes show long lifetimes [39].

As pyrene shows a T_1 state with similar energy to the emissive state of Pt–TPP, therefore, Pt–TPyP was investigated. First the geometries and the electronic structures of the TPyP were studied with similar approach. We found that the porphyrin core of TPyP adopts planar geometry. For the pyrene appendents, however,

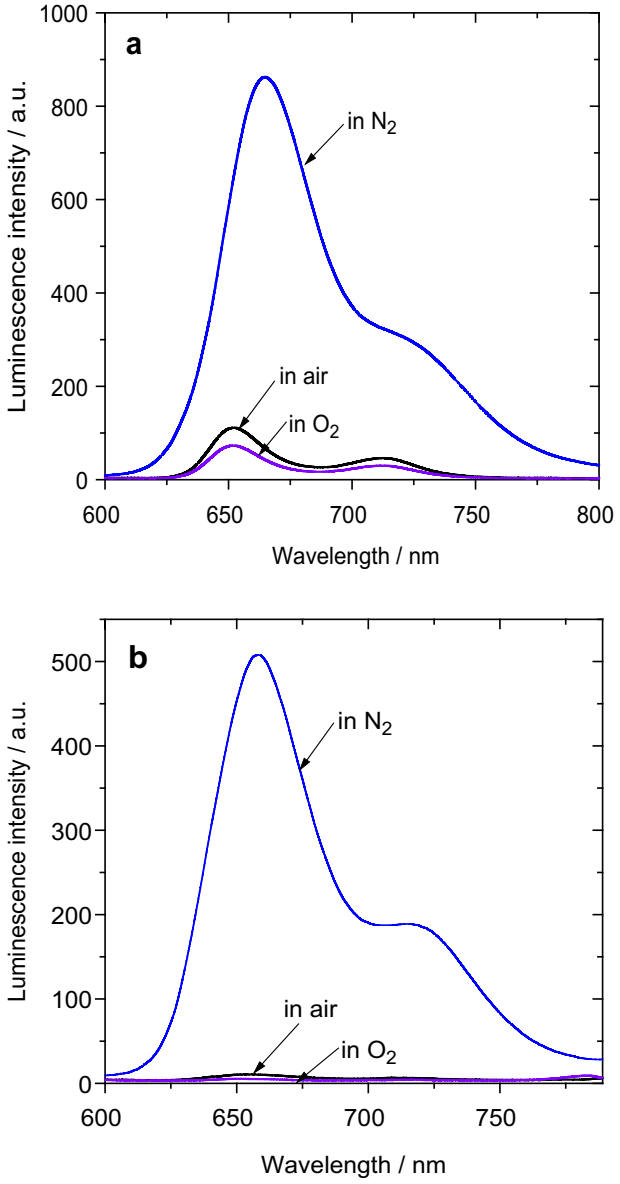

Fig. 6. Phosphorescent emission intensity of Pt complex solution saturated with nitrogen, air and oxygen. (a) Pt–TPP. Excitation wavelength λex = 416 nm I_0/I_{100} = 12.0. (b) Pt–TNP. Excitation wavelength λex = 414 nm I_0/I_{100} = 101.0. $c = 2.0 \times 10^{-6}$ mol/L of complexes in $CHCl_3$. 27 °C.

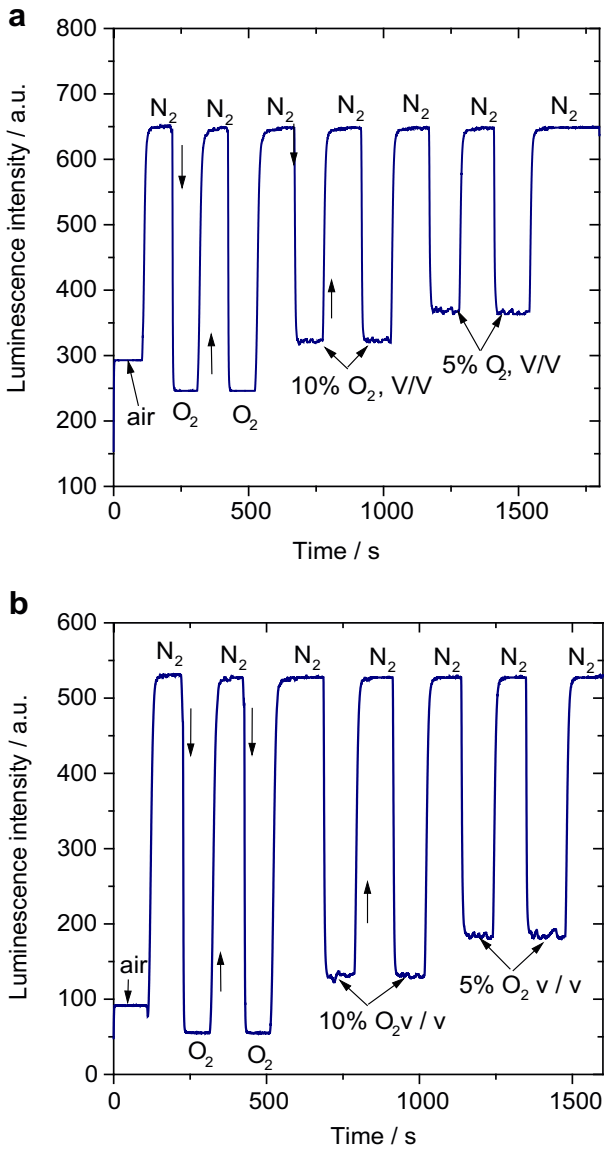

Fig. 7. Phosphorescent intensity response of sensing films of the Pt complexes of Pt–TPP and Pt–TNP in IMPEK-C to O_2/N_2 switching cycles, measured with home-assembled optical fiber/flow cell system. (a) Intensity response of the sensing film of Pt–TPP. λex = 425 nm; λem = 652 nm. (b) Intensity response of Pt–TNP sensing film. λex = 421 nm; λem = 658 nm.

a nearly perpendicular geometry were observed (Fig. 4, ca. 90°), probably due to the more significant steric hindrance of the pyrene units. Such geometry completely rules out the π-conjugation between the pyrene units and the porphyrin core. This postulation is supported by the UV–Vis absorption of the TPyP (Fig. 1a), which shows similar profile to that of TPP.

The electronic configurations of the excited states were investigated and we found that pyrene units do not involve in the low-lying electronic transitions (Fig. 4 and Table 4). The TDDFT calculation based on the ground state geometry show that the main UV–Vis absorption bands are located at 561 nm, 522 nm, 462 nm and 401 nm, respectively. For example, the $S_0 \rightarrow S_{11}$ transition shows an excitation energy of 401 nm, which is close to the experimental results of 434 nm. Pyrene units are involved in this transition (Table 4). Similar involvement of naphthal fragment in the S_3 state of TNP was found (see Supporting Information). For the S_1 state, however, no involvement of the aryl appendents was observed in the TDDFT calculations. Thus, we expect different absorption profile at 400 nm for the TPP, TNP and TPyP ligands. According to kasha's rule [11], the emission property will be similar as the S_1 state of the ligands share similar electronic structure (without any involvement of aryl appendents). The experimental results fully support these theoretical predictions (Fig. 1a).

For Pt–TPyP, however, we found pyrene units contribute to the electronic transitions, although to a minor extent (Fig. 5). We propose the involvement of the pyrene ligand in the electronic transitions may extend the luminescent lifetimes of the Pt complexes [12,40–48].

The geometries and the low-lying excited states of the TNP and Pt–TNP were also studied and similar results to TPyP and Pt–TPyP were found (see Supporting Information). Our theoretical calculations propose that there is no efficient delocalization for the MOs between the aryl appendents (such as phenyl, naphthyl and pyrenyl) and the porphyrin core. For example, DFT/TDDFT calculations indicate only minor involvement of the pyrene fragments in the low-lying excited states. These predictions were fully supported by the UV–Vis absorption and luminescence spectra of the ligands and the Pt complexes. These findings may prove useful in future design of dyad Pt–porphyrin complexes or study of the photophysical properties of the substituted porphyrins and the Pt(II) complexes.

The geometry of the complex Pt–TPyP was studied and it was found the metalation imparts minor effect on the geometry of the porphyrin core. For the electronic transitions, the MOs involved in the main transitions are basically located on the porphyrin core. The calculated transitions (496 nm, 386 nm 367 nm) are different from the TPyP ligand (Table 5), and these absorptions are in good agreement with the experimental observations.

3.4. Oxygen sensing performance of Pt complex in polymers

The luminescent O_2 sensing properties of the triplet emitters are strongly correlated to their unquenched luminescent lifetimes [8,12]. The O_2 sensing properties can be greatly improved by tuning the luminescence lifetimes [12,49]. We have found that the lifetime of the Pt complexes were tuned with the introduce of the aryl appendents at the meso position of the porphyrins (Table 1). This is probably due to the minor involvement of the pyrene units in the electronic transitions (Table 5 and Fig. 5).

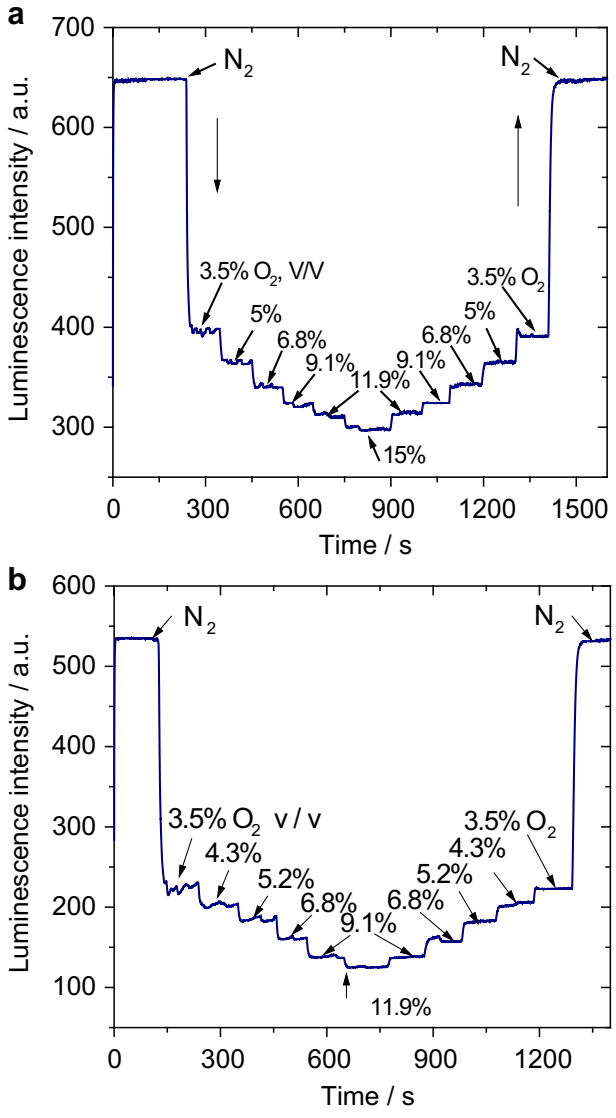

Fig. 8. Phosphorescent intensity response of sensing film in polymer IMPEK-C to step variations of O_2 concentrations, measured with home-assembled optical fiber/flow cell system. The numbers indicate the O_2 concentration in mixed O_2/N_2 gas (V/V). (a) Intensity response of Pt–TPP sensing film. λex = 425 nm; λem = 652 nm. (b) Intensity response of Pt–TNP. λex = 421 nm; λem = 658 nm.

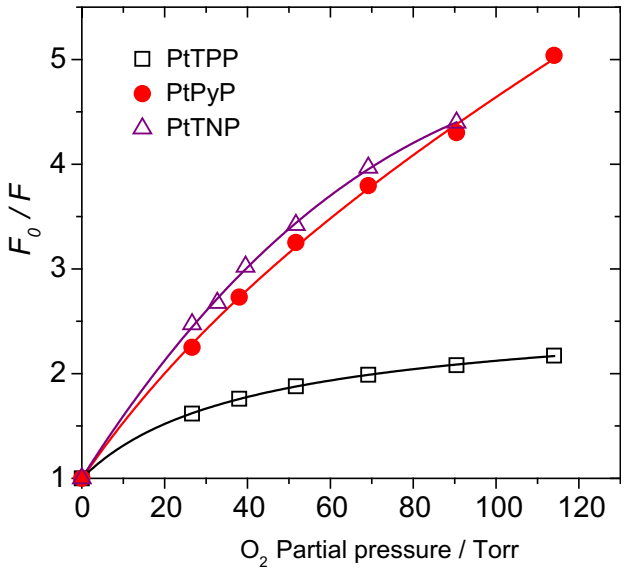

Fig. 9. Two-site model plots for sensing film of Pt porphyrin complexes Pt–TPP, Pt–TNP and Pt–TPyP in IMPEK-C. Intensity ratios F_0/F vs O_2 partial pressure (Torr).

Table 6
Parameters of O_2 sensing film of complex Pt–TPP, Pt–TPyP and Pt–TNP with IMPEK-C as supporting matrix (fitting result of the emission intensity with the two-site model).

	f_1[a]	f_2[a]	K_{SV1}[b]	K_{SV2}[b]	r^2[c]	K_{sv}^{appd}	pO_2[e]
Pt–TPP	0.60	0.40	0.066 ± 0.004	0.000 ± 0.000	1.000	0.040	25.3
Pt–TPyP	0.86	0.14	0.066 ± 0.019	0.003 ± 0.005	0.999	0.057	17.4
Pt–TNP	0.89	0.11	0.077 ± 0.014	0.000 ± 0.003	1.000	0.068	14.7

[a] The ratio of the two portion of the dyes.
[b] The quenching constants of the two portions.
[c] The determination coefficients.
[d] Weighted quenching constant, $K_{SV}^{app} = f_1 \times K_{SV1} + f_2 \times K_{SV2}$.
[e] The oxygen partial pressure at which the initial emission intensity of film is quenched by 50%, and can be calculated as $1/K_{SV}$.

The O_2 sensitivities of the emission of the complexes in solution were investigated (Fig. 6). For the Pt–TPP, it was found the emission intensity was quenched by ca. 12-fold in O_2 saturated solution, when compared to that in N_2 saturated solution (Fig. 6a). For the derivative of Pt–TNP, however, the emission intensity was reduced by ca. 101-fold in neat O_2 when compared to that in neat N_2 (Fig. 6b). The O_2 quenching effect on the emission of Pt–TPyP was studied and ca. 86-fold of quenching effect was observed (see Supporting Information). These quenching effects demonstrate that the Pt–TNP and Pt–TPyP complexes are characterized with longer emission lifetime than the model complex Pt–TPP, and the emission intensity of Pt–TPyP and Pt–TNP are much more sensitive to the presence of O_2. The lifetime values of the complexes support this postulation (Table 1).

The O_2 sensitivity of the complexes was also investigated in polymer films (IMPEK-C, poly(aryl ether ketone)) [7]. For the saturation cycles of N_2 and O_2 (Fig. 7), very short of response time ($t\downarrow 95$) and recovery time ($t\uparrow 95$) (time to finish 95% emission intensity change) of 4 s and 9 s were found for the complex Pt–TNP. For Pt–TPP, similar results ($t\downarrow 95$ and $t\uparrow 95$) of 2 s and 7 s were observed, respectively. Such fast response and recovery is ideal for practical luminescent oxygen sensors and usually can only be achieved with porous materials as the supporting matrix for the phosphorescent dyes, such as MCM-41 or Organogel [4,50–54]. Our preparation of the sensing film is straightforward, and it may prove useful for application in practical O_2 sensors.

Furthermore, we found the quenching of Pt–TNP in polymer film was more significant than that of Pt–TPP. For example, the emission intensity of Pt–TNP was quenched by 90% when switch from N_2 to O_2. For Pt–TPP, however, only 62% of quenching effect was observed (Fig. 7a). The different quenching effects indicate different luminescent lifetimes for the two complexes. This postulation was supported by the luminescent lifetime studies (Table 1).

In order to investigate the O_2 sensing property of the complexes quantitatively, the emission changes of the sensing films vs. small steps of O_2 partial pressure variation was studied (Fig. 8). We found both Pt–TPP and Pt–TNP sensing films are sensitive to low O_2 partial pressure. For example, the emission intensity of Pt–TPP was

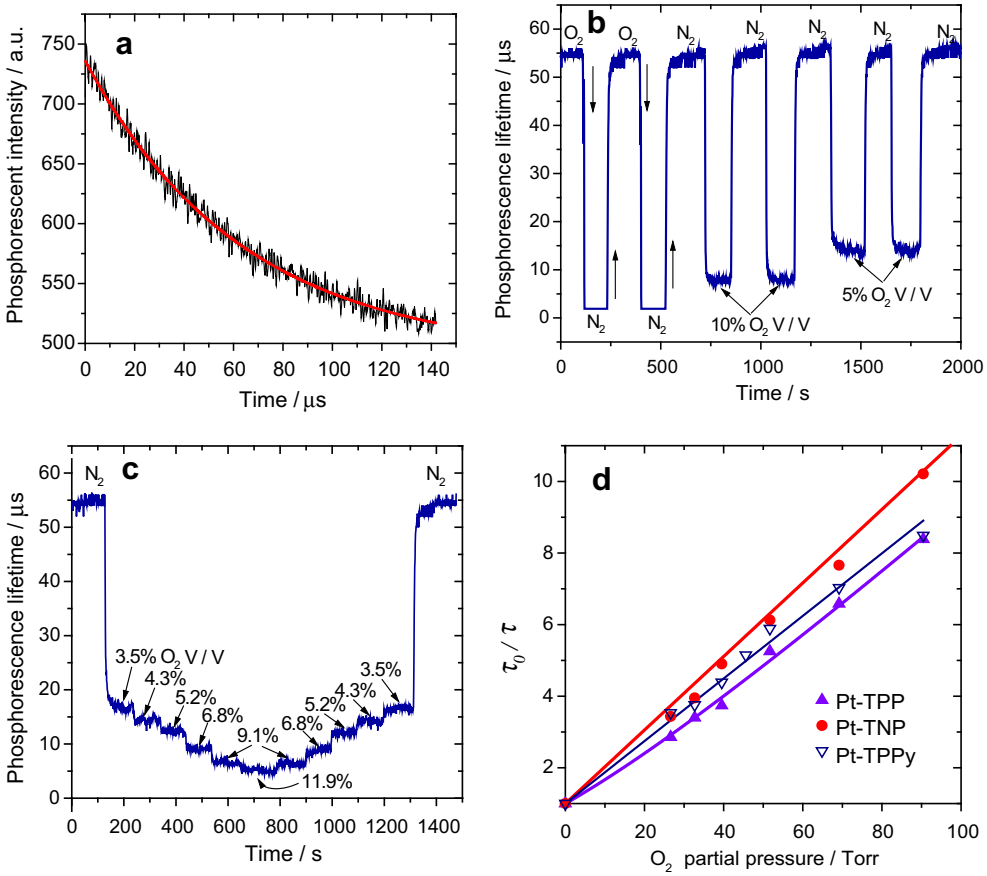

Fig. 10. Oxygen sensing property of the Pt–TPP polymer films monitored by the luminescence lifetime variation against the oxygen partial pressure changes. (a) Phosphorescence decay curve of Pt–TPP in IMPEK-C in neat N_2, Monoexponential decay regression gave lifetime $\tau = 54.7 \pm 0.9$ µs ($r^2 = 0.99$). (b) phosphorescence lifetime response of sensing film of Pt–TPP in IMPEK-C to O_2/N_2 saturation cycles and switch between neat N_2, 10% O_2 and 5% O_2 (V/V). (513 nm LED as excitation light source and the emission beyond 600 nm is used for the τ monitoring). (c) lifetime response of sensing film of TPP-Pt in IMPEK-C to step variation of O_2 concentration in O_2/N_2 mixture. (d) Fitting of the lifetimes-oxygen partial pressure with the two-site model.

Table 7
Parameters of O_2 sensing film of complex Pt–TPP, Pt–TPyP and Pt–TNP with IMPEK-C as supporting matrix (fitting result of the luminescent lifetime with the two-site model).

	f_1[a]	f_2[a]	K_{SV1}[b]	K_{SV2}[b]	r^2[c]	K_{sv}^{appd}	p_{O_2}[e]
Pt–TPP	0.56	0.44	0.080	0.080	0.99	0.080	12.6
Pt–TPyP	0.98	0.018	0.099	0.00	0.99	0.097	10.3
Pt–TNP	0.58	0.42	0.100	0.10	0.99	0.10	9.7

[a] The ratio of the two portion of the dyes.
[b] The quenching constants of the two portions.
[c] The determination coefficients.
[d] Weighted quenching constant, $K_{SV}^{app} = f_1 \times K_{SV1} + f_2 \times K_{SV2}$.
[e] The oxygen partial pressure at which the initial emission intensity of film is quenched by 50%, and can be calculated as $1/K_{SV}$.

quenched by 39.2% when switch from N_2 to 3.5% O_2 (mixture with N_2, V/V). Higher quenching extent (58.3%) was observed for Pt–TNP (Fig. 8b). For Pt–TPyP complex, the phosphorescent emission intensity was quenched by 43.5% under same conditions (see Supporting Information).

Different models have been used to describe the heterogeneous oxygen sensing, such as the modified Stern–Volmer equation, the two-site model, etc. [7,8]. Herein the oxygen sensing data (Fig. 8) were fitted with the two-site model (Fig. 9) [7]. The corresponding fitting data were summarized in Table 6. It was found the Pt–TNP and Pt–TPyP give higher quenching constants than the reference complex Pt–TPP. For example, the apparent quenching constant of Pt–TPP is 0.0396 $Torr^{-1}$, this value was improved to 0.0642 $Torr^{-1}$ for Pt–TNP. For Pt–TPyP film, the apparent quenching constant is 0.057 $Torr^{-1}$. Furthermore, the emission quenching efficiency was also improved for the Pt–TNP and Pt–TPyP than that of Pt–TPP. These results demonstrate that the luminescent oxygen sensing property can be improved with modification of the porphyrin core.

The above O_2 sensing studies were carried out by emission intensity monitoring. Lifetime monitoring is intrinsically superior [7]. Therefore, the lifetime changes of the Pt porphyrin complexes in polymer films were studied with our home-assembled time-domain lifetime device (which can record the lifetime changes of the sensing films against the variation of the O_2 partial pressures, as well as discreet decay curves) [7]. The phosphorescent decay curve of Pt–TPP after excitation (with green-light emitting LED as light source) was shown as Fig. 10a. Single-exponential fitting of the curve give lifetime of 54.7 ± 0.9 μs ($r^2 = 0.99$), which is very close to the reported value of 52 μs [31], validate our time-domain lifetime instrument.

Next, the lifetime changes of the sensing film of Pt–TPP were recorded and fast response and recovery were observed. The lifetime variation of the sensing film against small steps of O_2 partial pressure variation is also studied (Fig. 10c) and reasonable resolution was observed. The complexes Pt–TNP and Pt–TPyP were studied with the lifetime instrument and the fitting result of the O_2 sensing was presented as Fig. 10d. We found complex Pt–TNP is the most sensitive to O_2, a conclusion which is in agreement with the phosphorescence intensity study (Fig. 9). The O_2 sensing with the lifetime monitoring mode is also fitted with the two-site model (Table 7). These results show that the oxygen sensing properties of the phosphors with long luminescent lifetimes can be studied with the continuous lifetime monitoring methods.

4. Conclusions

In summary, we synthesized 5,10,15,20-tetraarylporphyrins (where aryl = phenyl, pyrenyl and naphthyl) and the corresponding Pt(II) complexes. The photophysical properties of the porphyrin ligands and the Pt(II) complexes were studied with UV–Vis absorption and photo-luminescence spectra. These ligands (or complexes) give similar absorption and emission profiles, indicating that there is no significant electronic communication (such as π-conjugation) between the aryl substitutions and the porphyrin core. The geometries and the electronic structure of the ligands and the complexes were studied with DFT/TDDFT calculations, which support the proposed weak electronic communications of the aryl appendents and the porphyrin core. The luminescent oxygen sensing properties of the Pt(II) complexes were studied in solution as well as in polymer films. The results demonstrated that with introducing of pyrenyl or naphthyl appendents, the O_2 sensing property of the complexes improved by 1.7 fold (Stern–Volmer quenching constant $K_{sv} = 0.040$ $Torr^{-1}$ for the reference complex Pt–TPP, compared to the complex Pt–TNP, $K_{sv} = 0.068$ $Torr^{-1}$). Our study of the photophysical properties of the porphyrins and the Pt (II) complexes may prove useful for future design of porphyrins and Pt porphyrin complexes as functional materials, such as light harvesting or photodynamic therapeutic reagents.

Acknowledgment

We thank the NSFC (20642003, 20634040 and 20972024), Ministry of Education (SRF for ROCS, SRFDP-200801410004 and NCET-08-0077), PCSIRT(IRT0711), State Key Laboratory of Fine Chemicals (KF0710 and KF0802), State Key Laboratory of Chemo/Biosensing and Chemometrics (2008009), the Education Department of Liaoning Province (2009T015) and Dalian University of Technology (SFDUT07005 and 1000-893394) for financial support.

Appendix. Supplementary data

Supplementary data associated with this article can be found, in the online version, at doi:10.1016/j.dyepig.2010.01.020.

References

[1] Wolfbeis O, Narayanaswamy R. Optical sensors: industrial, environmental and diagnostic applications. Anal Bioanal Chem 2005;381:18–9.
[2] (a) Goui JF, Bares F, Birot D, André JC. A fibre-optic oxygen sensor for oceanography. Sens Actuators B 1997;38–39:401–6;
(b) López-Gándara C, Ramos FM, Cirera A, Cornet A. A model of the behavior of the limiting current oxygen sensors. Sens Actuators B 2009;140:432–8.
[3] Chu C, Lo Y. High-performance fiber-optic oxygen sensors based on fluorinated xerogels doped with Pt (II) complexes. Sens Actuators B 2007;124:376–82.
[4] Basu BJ. Optical oxygen sensing based on luminescence quenching of platinum porphyrin dyes doped in ormosil coatings. Sens Actuators B Chem 2007; 123:568–77.
[5] Xin L, Mitchell AW. Luminescence quenching in polymer/filler nanocomposite films used in oxygen sensors. Chem Mater 2001;13:3449–63.
[6] Victor VV, Sergey MB. Optical oxygen sensors based on phosphorescent water-soluble platinum metals porphyrins immobilized in perfluorinated ion-exchange membrane. Sens Actuators B 2002;82:272–6.
[7] Ji SM, Wu WH, Wu YB, Zhao T, Zhou FK, Yang YB, et al. Real-time monitoring of luminescent lifetime changes of PtOEP oxygen sensing film with LED/photodiode-based time-domain lifetime device. Analyst 2009;134:958–65.
[8] Lakowicz JR. Principles of fluorescence spectroscopy, seconded. New York: Kluwer Academic/Plenum Press; 1999.
[9] Wolfbeis O, Narayanaswamy R. Optical sensors: industrial, environmental and diagnostic applications. Berlin-Heidelberg: Springer-Verlag; 2004.
[10] Wang Z, Chen T, Xu J. Gas and water vapor transport through a series of novel poly (aryl ether sulfone) membranes. Macromolecules 2001;34:9015–22.
[11] Valeur B. Molecular fluorescence: principles and applications. Wiley-VCH Verlag GmbH; 2001.
[12] Harriman A, Khatyr A, Ziessel R. Extending the luminescence lifetime of ruthenium (II) poly (pyridine) complexes in solution at ambient temperature. Dalton Trans; 2003:2061–8.
[13] (a) Wang X, Guerzo AD, Schmehl RH. Photophysical behavior of transition metal complexes having interacting ligand localized and metal-to-ligand charge transfer states. J Photochem Photobiol C 2004;5:55–7;
(b) Nguyen KA, Kennel J. A density functional theory study of phosphorescence and triplet–triplet absorption for nonlinear absorption chromophores. J Chem Phys 2002;117:7128–35.

[14] McClenaghan ND, Leydet Y, Maubert B, Indelli MT, Campagna S. Excited-state equilibration: a process leading to long-lived metal-to-ligand charge transfer luminescence in supramolecular systems. Coord Chem Rev 2005;249:1336–50.
[15] Papkovsky DB, O'Riordan TC. Emerging applications of phosphorescent metalloporphyrins. J Fluoresc 2005;15(4):569–84.
[16] Wang Z, Chen T, Xu J. Gas transport properties of novel cardo poly(aryl ether ketone)s with pendant alkyl groups. Macromolecules 2000;33:5672–9.
[17] (a) Lin W, Long L, Feng J, Wang B, Guo C. Synthesis of *meso*-coumarin-conjugated porphyrins and investigation of their luminescence properties. Eur J Org Chem 2007;26:4301–4;
(b) Che C, Hou Y, Chan M, Chan W, Guo J, Liu Y, et al. [meso-Tetrakis(pentafluorophenyl) porphyrinato]platinum(II) as an efficient, oxidation-resistant red phosphor: spectroscopic properties and applications in organic light-emitting diodes. J Mater Chem 2003;13:1362–6.
[18] Frisch MJ, Trucks GW, Schlegel HB, Scuseria GE, Robb MA, Cheeseman JR. Gaussian 09, revision A. l. Wallingford CT: Gaussian, Inc.; 2009.
[19] Zhang Y, Yang R, Liu F, Li KA. Fluorescent sensor for imidazole derivatives based on monomer-dimer equilibrium of a zinc porphyrin complex in a polymeric film. Anal Chem 2004;76:7336–45.
[20] Yang Y, Ji S, Zhou F, Zhao J. Synthesis of novel bispyrene diamines and their application as ratiometric fluorescent probes for detection of DNA. Biosens Bioelectron 2009;24:3442–7.
[21] Sheng N, Zhu P-H, Ma C-Q, Jiang J-Z. The synthesis, spectroscopy, electrochemistry and photophysical properties of novel, sandwich europium(III) complexes with a porphyrin ligand bearing four pyrenyl groups in meso-positions. Dyes Pigm 2009;81:91–6.
[22] Guo J, Ye K, Wu Y, Liu Y, Yue W. Red electroluminescent devices based on a porphyrin metal complex. Synth Met 2003;137:1075–6.
[23] Baker GA, Bright FV, Detty MR, Pandey S, Stilts CE, Yao H. The influence of phenylethynyl linkers on the photo-physical properties of metal-free porphyrins. J Porphyr Phthalocyanines 2000;4:669–83.
[24] Fonda HN, Gilbert JV, Cormier RA, Sprague JR, Kamioka K, Connolly JS. Spectroscopic, photophysical, and redox properties of some meso-substituted free-base porphyrins. J Phys Chem 1993;97:7024–33.
[25] Mathew S, Johnston MR. The synthesis and characterisation of a free-base porphyrin–perylene dyad that exhibits electronic coupling in both the ground and excited states. Chem Eur J 2009;15:248–53.
[26] Mondal JA, Ramakrishna G, Singh AK, Ghosh HN, Mariappan M, Maiya BG, et al. Ultrafast intramolecular electronic energy-transfer dynamics in a bichromophoric molecule. J Phys Chem A 2004;108:7843–52.
[27] Harriman A, Hissler M, Khatyr A, Ziessel R. A ruthenium(ii) *tris*(2,2A-bipyridine) derivative possessing a triplet lifetime of 42 μs. Chem Commun 1999;8:735–6.
[28] Kozlov DV, Tyson DS, Goze C, Ziessel R, Castellano FN. Room temperature phosphorescence from ruthenium (II) complexes bearing conjugated pyrenylethynylene subunits. Inorg Chem 2004;43:6083–92.
[29] Goze C, Kozlov DV, Tyson DS, Ziessel R, Castellano FN. Synthesis and photophysics of ruthenium(II) complexes with multiple pyrenylethynylene subunits. New J Chem 2003;27:1679–83.
[30] Li L, Zhang Z, Long W, Tong A. Study of properties on non-protected room temperature phosphorescence and delayed excimer fluorescence of pyrene solution. Spectrachim Acta Part A 2001;57:385–93.
[31] Finikova OS, Chen P, Ou Z, Kadish KM, Vinogradov SA. J Photochem Photobio A Chem 2008;198:75–84.
[32] Ren X, Ren A, Feng J, Sun C. A density functional theory study on photophysical properties of red light-emitting materials: meso-substituted porphyrins. J Photochem and Photobio A Chem 2009;203:92–9.
[33] Liu Y, Feng J, Ren A. A density functional theory study on photophysical properties of red light-emitting materials: meso-substituted porphyrins. J Phys Chem A 2008;112:3157–64.
[34] Vlček Jr A, Záliš S. , Modeling of charge-transfer transitions and excited states in d^6 transition metal complexes by DFT techniques. Coord Chem Rev 2007;251:258–87.
[35] Anders Borg O, Godinho S, Lundqvist M, Lunell S, Persson P. Computational study of the lowest triplet state of ruthenium polypyridyl complexes used in artificial photosynthesis. J Phys Chem A 2008;112:4470–6.
[36] Zhao G, Liu J, Zhou L, Han K. Site-selective photoinduced electron transfer from alcoholic solvents to the chromophore facilitated by hydrogen bonding: a new fluorescence quenching mechanism. J Phys Chem B 2007; 111:8940–5.
[37] Han F, Chi L, Liang X, Ji S, Liu S, Zhou F, et al. 3,6-Disubstituted carbazole-based bisboronic acids with unusual fluorescence transduction as enantioselective fluorescent chemosensors for tartaric acid. J Org Chem 2009;74:1333–6.
[38] Ji S, Yang J, Yang Q, Liu S, Chen M, Zhao J. Tuning the Intramolecular charge transfer of alkynylpyrenes: effect on photophysical properties and its application in design of OFF–ON fluorescent thiol probes. J Org Chem 2009;74:4855–65.
[39] Zhou G, Wang Q, Wong W, Ma D, Wang L, Lin Z. A versatile color tuning strategy for iridium(III) and platinum(II) electrophosphors by shifting the charge-transfer states with an electron-deficient core. J Mater Chem 2009;19:1872–83.
[40] Wilson GJ, Launikonis A, Sasse WHF, Mau AW-H. Excited-state processes in ruthenium(II) bipyridine complexes containing covalently bound arenes. J Phys Chem A 1997;101:4860–6.
[41] Tyson DS, Castellano FN. Intramolecular singlet and triplet energy transfer in a ruthenium(ii) diimine complex containing multiple pyrenyl chromophores. J Phys Chem A 1999;103:10955–60.
[42] Tyson DS, Bialecki J, Castellano FN. Ruthenium(II) complex with a notably long excited state lifetime. Chem Commun 2000;23:2355–6.
[43] Tyson DS, Henbest KB, Bialecki J, Castellano FN. Excited state processes in ruthenium(II)/pyrenyl complexes displaying extended lifetimes. J Phys Chem A 2001;105:8154–61.
[44] Guerzo AD, Leroy S, Fages F, Schmehl RH. Photophysics of Re(I) and Ru(II) diimine complexes covalently linked to pyrene: contributions from Intraligand charge transfer states. Inorg Chem 2002;41:359–66.
[45] Morales AF, Accorsi G, Armaroli N, Barigelletti F, Pope SJA, Ward MD. Interplay of light antenna and excitation "Energy reservoir" effects in a bichromophoric system based on ruthenium-polypyridine and pyrene units linked by a long and flexible poly(ethylene glycol) chain. Inorg Chem 2002;41:6711–9.
[46] De Carvalho IMM, Moreiraí De Sousa, Gehlen MH. Synthesis, characterization, and photophysical studies of new bichromophoric ruthenium (II) complexes. Inorg Chem 2003;42:1525–31.
[47] Maubert B, McClenaghan ND, Indelli MT, Campagna S. Absorption spectra and photophysical properties of a series of polypyridine ligands containing appended pyrenyl and anthryl chromophores and of their ruthenium(II) and osmium(II) complexes. J Phys Chem A 2003;107:447–55.
[48] Simon JA, Curry SL, Schmehl RH, Schatz TR, Piotrowiak P, Jin XQ, et al. Intramolecular electronic energy transfer in ruthenium(II) diimine donor/pyrene acceptor complexes linked by a single C–C bond. J Am Chem Soc 1997; 119:11012–22.
[49] Mak CSK, Pentlehner D, Stich M, Wolfbeis OS, Chan WK, Yersin H. Exceptional oxygen sensing capabilities and triplet state properties of Ir(ppy-NPh_2)$_3$. Chem Mater 2009;21:2173–5.
[50] Leventis N, Rawashdeh AMM, Elder IA, Yang J, Dass A, Sotiriou-Leventis C. Synthesis and characterization of ru(ii) tris(1,10-phenanthroline)-electron acceptor dyads incorporating the 4-benzoyl- *N*-methylpyridinium cation or *N*-benzyl-*N*-methyl viologen. Improving the dynamic range, sensitivity, and response time of sol–gel-based optical oxygen sensors. Chem Mater 2004;16:1493–506.
[51] Lei B, Li B, Zhang H, Lu S, Zheng Z, Li W, et al. Mesostructured silica chemically doped with Ru^{II} as a superior optical oxygen sensor. Adv Funct Mater 2006;16:1883–91.
[52] Zhang H, Sun Y, Ye K, Zhang P, Wang Y. Oxygen sensing materials based on mesoporous silica MCM-41 and Pt(II)–porphyrin complexes. J Mater Chem 2005;15:3181–6.
[53] Wang B, Liu Y, Li B, Yue S, Li W. Optical oxygen sensing materials based on trinuclear starburst ruthenium(II) complexes assembled in mesoporous silica. J Lumin 2008;128:341–7.
[54] Yeh TS, Chu CS, Lo YL. Highly sensitive optical fiber oxygen sensor using Pt(II) complex embedded in sol–gel matrices. Sens Actuators B Chem 2006; 119:701–7.